A new method for determination of *Thy1*-GCaMP6s using two-photon microscopy in mice

Shutaro Kobayashi

Nihon University Graduate School of Dentistry,

Major in Oral and Maxillofacial Surgery I

(Directors: Profs. Morio Tonogi, Masayuki Kobayashi, and Satoshi Fujita)

Index

This thesis is composed of the following article and the additional result showing the reduction of the intensity of green fluorescence in the cross-sectioned tail after 24 h (Fig. 5).

Kobayashi S, O'Hashi K, Kaneko K, Kobayashi S, Ogisawa S, Tonogi M, Fujita S, and Kobayashi M (2022) A new phenotype identification method with the fluorescent expression in cross-sectioned tails in *Thy1*-GCaMP6s transgenic mice. J Oral Sci, in press.

Abstract

Purpose: Unless the phenotype of the transgenic mice is distinguishable, genotyping in each mouse is required prior to following experiments. This study aimed to establish a new identification method for the phenotype in *Thy1*-GCaMP6s transgenic mice to reduce the cost and time.

Methods: Tail biopsies (2 mm) were performed under general anesthesia with isoflurane at 3-4 weeks old mice. Then, the resected tail was cut again with a sharp razor, and the tail cross-sections and the cerebral cortex were observed with two-photon microscopy (excitation wavelength = 940 nm). The emitted light was split into green and red light by a dichroic mirror (570 nm) with bandpass filters (495-540 nm for green, 575-645 nm for red).

Results: Two types of the expressed fluorescent pattern were found in the tail tissue: the mouse with the green fluorescent structures (type 1) and the mouse without those (type 2). Cortical imaging confirmed that type 1 expressed the cortical GCaMP6s, while type 2 did not.

Conclusion: These results suggest that observation of the cross-sectioned tail in *Thy1*-GCaMP6s mice enabled to identify the phenotype quickly, which reduces the cost and time for genotyping.

Introduction

In calcium imaging, calcium indicators visualize cellular activities accompanied by changing intracellular calcium concentration [1-3]. Using two-photon microscopy, the neural activities in many neurons in the field of view can be simultaneously measured in a non-invasive manner [4-8]. Recently, genetically encoded calcium indicators (GECIs) such as the GCaMP6 series have been developed and are widely used [2,7,9]. There are various gene delivery methods to express GECIs, e.g. viral infection and electroporation, the transgenic methods have an advantage in stable expression of GECIs without invasive procedures [3,10].

GCaMP6s is a green fluorescent calcium protein indicator, and the fluorescence intensity potently rises in response to an increase in the intracellular calcium concentration, such as action potentials in neurons [2,3,7]. *Thy1*-GCaMP6s transgenic mice have been developed by transgenic methods and express GCaMP6s under the *Thy1* promoter, in which projection neurons in the cerebral cortex and hippocampus express GCaMP6s [3]. In the breeding of this strain, hemizygotes are viable and fertile [https://www.jax.org/strain/024275]. Therefore, prior to the calcium imaging experiment, it is necessary to identify the phenotype in each mouse, i.e. presence or absence of GCaMP6s expression. However, a craniotomy to identify cortical GCaMP6s expression is invasive and likely to be as inappropriate method.

In addition to neurons in the brain, some or all peripheral sensory and motor axons are regulated by elements from the *Thy1* gene in mice [11-13]. Since the expression patterns of fluorescent proteins under the *Thy1* promoter in transgenic mice

are varied in comparison among several transgenic mice strains [3,11,14], it is still unclear whether there are some structures with GCaMP6s expressions in the peripheral tissue of *Thy1*-GCaMP6s transgenic mice. Currently, genotyping is performed to distinguish the hemizygotes and non-carriers for the GCaMP6s DNA sequences in each mouse. Typically, the PCR assays are performed to genotype, which requires articles of consumption and time to obtain the results [https://www.jax.org/strain/024275]. The tail biopsy is one of the popular methods to obtain a tissue sample for PCR [15-17]. In this study, structures expressing GCaMP6s in the cross-sectioned tails of *Thy1*-GCaMP6s transgenic mice were explored to examine the possibility whether fluorescence observation of the tail section can be used to identify the GCaMP6s.

Materials and Methods

Animals

The Animal Experimentation Committee of Nihon University approved the experiments (AP16D028, AP16D029, AP17D003, AP18DEN024, AP18DEN047, AP19DEN025). Experiments were performed according to the institutional guidelines for the care and use of experimental animals described in the National Institutes of Health Guide for the Care and Use of Laboratory Animals. All efforts were made to minimize animal suffering and to reduce the number of animals used.

Male *Thy1*-GCaMP6s transgenic mice (hemizygous for Tg(*Thy1*-GCaMP6s)GP4.3Dkim, C57BL/6J-Tg(*Thy1*-GCaMP6s)GP4.3Dkim/J, Jax #024275)[2] were obtained from Jackson Laboratories [http://jaxmice.jax.org]. Subsequently, the transgenic strain was maintained by mating the male hemizygous mouse to a female wild-type mouse (C57BL/6J, Charles River Japan, Yokohama, Japan).

Observation of cross-sectioned tail

Until the day of the tail biopsy, the offspring and dam were housed in a single cage. Tail biopsies in the offspring were performed 3-4 weeks postpartum. The mouse was anesthetized with 4.0% isoflurane (inhalation), and the tail transection with a sharp razor blade was performed (2 mm, the first cut; Fig. 1A, left). After the arrest of bleeding, ropivacaine hydrochloride (AstraZeneca, Osaka, Japan), a long-lasting local anesthetic, was applied to the incision. Then, the resected tail was cut with a sharp razor

blade in half (1 mm, the second cut; Fig. 1A, right). Due to the vital reaction, the blood was attached to the plane obtained by the first cut, whereas there was little in the plane obtained by the second cut. As standard protocol, the tail section was fixed to a plastic dish with the second cut side facing up with super glue (Aron Alpha A, Daiichi-Sankyo, Tokyo, Japan). After the glue had hardened, the cross-sectioned tail was observed using a laser-scanning microscope system (FVMPE-RS, Olympus, Tokyo, Japan) equipped with an upright microscope (BX63, Olympus), a 25 × water immersion objective (N.A. = 1.05; XLPLN25XWMP2, Olympus), and a pulsed laser (Insight DS Dual-OL, Spectra-Physics, Santa Clara, CA, USA).

The images were obtained with a view consisting of 512 × 512 pixels (excitation wavelength = 940 nm). The emitted light was split into red and green light by a dichroic mirror (570 nm) with bandpass filters (495-540 nm for green, 575-645 nm for red; FV30-FGR, Olympus). The offspring were separated by sex and phenotype, i.e. presence (type 1) or absence (type 2) of some structures exhibited high green fluorescence in overlapped structures. Several cross-sectioned tails identified as type 1 were stored in a cool dark place (3℃) and were observed again using the laser microscope system 24 hours later. Subsequently, some mice were provided to other imaging experimental projects.

Observation of cerebral cortex

The mouse was prepared according to previous study [18]. Briefly, the mouse received an injection of methylatropine bromide (0.1-5 mg/kg, i.p., European Pharmacopoeia Reference Standard) and was anesthetized with urethane (1.4-1.7 g/kg, i.p., Sigma-Aldrich, St. Louis, MO, USA). The body temperature was maintained at

approximately 37 ℃ using a heating system (BWT-100, Bio Research Center, Osaka, Japan). The mouse was fixed to a custom-made stereotaxic snout frame, which was tilted 90° laterally for imaging the insular cortex. After subcutaneous injection of ropivacaine, the temporal muscle and zygomatic arch were carefully removed. A craniotomy (diameter = 0.5-4.0 mm) was performed to expose the cortical surface. Then, the imaging was performed using two-photon microscopy with the same settings as the cross-sectioned tail observation. Some mice identified as type 2 were euthanized by carbon dioxide inhalation, and the brains were removed and were imaged using two-photon microscopy to confirm the absence of GCaMP6s expression in the cerebral cortex.

Histology of the cross-sectioned tail

After the imaging, the cross-sectioned tail was fixed with 4.0% formalin and embedded in paraffin. Transverse sections were stained with hematoxylin and eosin (H-E) for detailed examination of tissue structures.

Data analysis

Data analysis was conducted with custom-written code in Matlab (Mathworks, Natick, MA, USA). To qualitatively identify GCaMP6s expression of the cross-sectioned tail, the divided green and red images were merged into one image. Resultant only greenish pixels indicate the presence of GCaMP6s expression, while resultant orangish pixels, i.e. mixed green and red, indicate the absence. For the quantitative evaluation of GCaMP6s expression, differential pixel values obtained by subtracting the raw brightness value of red fluorescent signals from those of green at the identical pixel locations were used.

These measures were defined as differential values, whose unit was the arbitrary unit (arb. unit). The larger positive differential value depicts the high level of GCaMP6s expression. To evaluate the cortical GCaMP6s expression, the change in fluorescent signals with depth was analyzed. First, depth-dependent fluorescent changes were corrected by eliminating the signal trend. The resultant signals were then represented as the fractional change (*dF/F*). Finally, mean calcium signals were obtained by averaging each image.

Statistical Analysis

N and *n* indicate the number of mice and images, respectively. The Wilcoxon signed-rank test was used in paired samples; otherwise, the Mann–Whitney *U* test was adopted under statistical comparison. For all comparisons, $P < 0.05$ was considered to be significant.

Results

Two types of fluorescent pattern in the cross-sectioned tail

The tail was cut twice to make the tail preparation for observation using two-photon microscopy (Fig. 1). The attached blood was found in the plane obtained by the first cut, whereas the plane obtained by the second cut had only a small amount of blood (Fig. 1A). There were two types of fluorescent patterns in the cross-sectioned tail. A typical example is shown in Fig. 1B,C. A large part of the structures with green fluorescence were overlapped to those with red. In addition to the overlapped structures, merged images showed that some structures exhibited green fluorescence only (Fig. 1B). However, some mice showed that all structures with green fluorescence were completely matched to those with red (Fig. 1C). The former and latter were defined as type 1 and type 2, respectively. The differential images revealed that the structures with high green intensity were specific in type 1. These results suggest that the difference of fluorescent patterns in the cross-sectioned tail could be the potential cue to identify whether or not the GCaMP6s expresses in the cortex.

Structured tail green-fluorescence relates to cortical GCaMP6s expression

Since the structured tail green-fluorescence patterns were visualized by the difference of fluorescent intensity between green and red images, this study attempted to establish an objective criterion for classifying fluorescent type to each mouse. The number of pixels exceeding the differential values in the range 10-100 was counted in all cross-sectioned images (N = 86; Fig. 2A). There were two groups of traces to the counted number of

pixels, for each of which tail images subjectively identified as type 1 (red) or type 2 (blue) of the fluorescent pattern were respectively included. Repetitive application of k-means clustering at each differential value revealed that the categorized results were stable at differential values from 30 to 70 (area shaded in cyan). Figure 2B shows one of the screened results obtained at 50 in the differential value, depicting the two divided distributions corresponding to type 1 (red) and type 2 (blue) fluorescent patterns. Thus, the screening result for each mouse is rigid, although the shape of the two distributions could somewhat change.

Next, how the type of fluorescent patterns in the cross-sectioned tail relates to cortical GCaMP6s expression by performing two-photon imaging on the cerebral cortex of the screened mice was investigated. Clear fluctuation of green fluorescence was detected from the cortical parenchyma and neurons from mice screened as type 1. In contrast, no apparent fluorescence was identified from those determined as type 2, although some stuck small faint fluorescence was observed (Fig. 2C). To confirm whether the detected fluorescence was attributed to neuronal activity, the depth transition of spontaneous cortical fluorescent signals was analyzed in both screened animals (Fig. 2D). The depth profile of averaged fluorescence from type 1 demonstrates the drastic change of the signals. On the other hand, signals from type 2 are stable, meaning that the detected faint fluorescence is derived from the autofluorescence of some cortical structures. Examples of the depth profiles from two types are shown in Fig. 2D. Their depth fluorescent transition is statistically significant ($n = 301$, $P < 0.001$, Mann–Whitney U test). These results indicate that type 1 and type 2 in the fluorescent patterns are GCaMP6s positive and negative, respectively.

Thus, GCaMP6s positive mice were able to be screened based on the

fluorescent intensity of the cross-sectioned tail. However, it remains unclear whether the intensity of the tail fluorescence correlates to that of the cortical fluorescence. To answer this question, a linear regression between the tail and cortical fluorescent intensities was conducted. The analysis showed no significant relationship between their intensities ($F(1, 9) = [1.44]$, $P = 0.26$; Fig. 2E). In this regard, although the tail fluorescence is not enough to predict the degree of the cortical GCaMP6s expression, it works well to detect the expression, as conventional PCR-based genotyping does.

Attached blood as a factor inhibiting correct genotyping

Screening the cortical GCaMP6s expression by detecting the fluorescence of the cross-sectioned tail is accessible and rigorous. However, the practical assessment for the expression was only derived from the preparation without attached blood. Figure 3 shows type 1 example, while the sample with blood on the sectioned-plane could yield a different result with artifacts, exhibiting less fluorescence intensity (Fig. 3B). To clarify the effects of the reduction of fluorescence intensity by the blood, the number of pixels regarded as fluorescence-positive in the samples without blood and with blood were compared. The attached blood significantly reduced the fluorescence intensity, leading to less patterned structure ($N = 9$, $P < 0.01$, Wilcoxon signed-rank test; Fig. 3C). These results indicate that blood-free preparation is necessary to avoid false-negative identification.

Structure of the detected fluorescence in the cross-sectioned tail

It was proved that green fluorescence in the cross-sectioned tail could be a cue for the cortical GCaMP6s expression. To explore the structures with green fluorescence in the

tail, two-photon tissue imaging was conducted using moxifloxacin as a contrast agent for tissues [19] after the tail imaging. As a result, some tissue structures such as tail bone, epidermis, hair follicle, and muscle within the section were identified (Fig. 4A)[20]. Superimposing the green fluorescent image (Fig. 4B) on the tissue image revealed that the fibrous structures emitting strong green fluorescence were located between the muscle and bone, suggesting that they were peripheral nerves positioned along with the tail bone. Additional H-E staining on the section from the imaged sample indicated that the fluorescent structures involved peripheral nerve tissues (Fig. 4C).

Confirmation in the cortical neurons

In mice identified as type 1 by observing the cross-sectioned tail, calcium imaging experiments that involved other experimental projects were also performed (N = 212). Consistent with the tail observation phenotype, cortical neurons expressed GCaMP6s. In addition, imaging in the living state (N = 3) and in the removed brain after euthanasia (N = 17) was performed in mice identified as type 2. There were no cortical neurons with GCaMP6s expression in type 2.

Reduction of the intensity of green fluorescence in the 24 h-stored cross-sectioned tail

Although the green fluorescence in the cross-sectioned tails of type 1 was visible several minutes after tail resection, the visuality could be varied with time. To confirm the possibility, I compared the image obtained minutes after the tail biopsy to that obtained 24 h later. As a result, the intensity of green fluorescence in the cross-sectioned tails was reduced 24 h after the tail resection (N = 5; Fig. 5).

Discussion

In this study, tail tissue regarding the presence and absence of green light fluorescent structures was investigated. The presence of green fluorescent structures in type 1 was clearly visible in the merged images in two-photon microscopy imaging. These phenotypes identified by observing the cross-sectioned tail were consistent with GCaMP6s expression in the cortical neurons. These results suggested that the observation of cross-sectioned tails can be a potent tool to identify the phenotype in *Thy1*-GCaMP6s transgenic mice, which enabled to reduce the cost and time required in genotyping.

Since the blood reduces the detected fluorescence intensity (Fig. 3), the preparation without blood is key to avoiding incorrect phenotype identification. The plane obtained by the first cut was attached with blood. Before the first cut, the vessels of the tail are dilated by blood pressure. Immediately after the first cut, the filled blood could be pushed out to the cut plane by the vessel contraction due to the blood pressure loss and vascular spasms in response to injury [21]. By cutting twice, the attached blood was able to be reduced.

GCaMP6s is a green fluorescent calcium indicator, and the elevation of intracellular calcium concentration potently increases the fluorescence intensity [2,3,7]. However, the intensity is relatively weak in inactive neural structures, i.e. low intracellular calcium concentration [2,3,7,22,23]. In this study, the green fluorescent structures in the cross-sectioned tail were clearly visible. This suggested that the intracellular calcium concentration in the green fluorescent structures was high. Some or

all peripheral sensory and motor axons are regulated by elements from the *Thy1* gene in mice [11-13]. The cut injured the nerve fibers running at the tip of the tail. It is reported that axonal injury dramatically increases intra-axonal calcium levels immediately after injury [24]. In addition, anoxia might also increase in the intracellular calcium concentration [25-27]. Thus, tail cut-induced increasing intracellular calcium concentration could increase the intensity of green fluorescence without specific treatments on the cut tail. The visibility was degraded in the cross-sectioned tails which were stored in cool dark place for 24 h (Fig. 5). Therefore, the observation of cross-sectioned tails should be performed quickly after the tail biopsy to avoid false-negative identification. From tissue two-photon imaging and H-E staining, parts of green fluorescent structures are likely to be peripheral nerves. It is known that there are other cells, e.g. epidermal cells, expressing *Thy1* in mice [28]. Actually, the intensity of green fluorescence around hair follicles is slightly high. Therefore, the possibility that cells expressing the green fluorescence include cells other than peripheral neurons is still remained.

In this study, tails to identify the phenotype of mice were used. The required amount of tail was equivalent to the amount used in PCR, and the invasiveness was not increased compared with general genotyping methods. Some articles of consumption were required in genotyping, and it takes time to get results [15-17]. On the other hand, this new phenotype identification method enabled to reduce the cost, and the result of phenotype could be obtained quickly.

These results suggested that phenotypes identified by observation of the cross-section of the tail can be a potent tool in identifying phenotype in *Thy1*-GCaMP6s transgenic mice, which enabled to reduce the cost and time required in genotyping. The

expression patterns of fluorescent proteins, including the GCaMP6 series, under the *Thy1* promoter vary among several transgenic mice strains [3,11]. This study investigated the GENIE Project4.3 mouse strain and did not assess other strains. Therefore, the possibility that this new identification method is unavailable in all other *Thy1*-GCaMP transgenic mouse strains is still remained. This issue should be addressed in future studies.

Acknowledgments

I am grateful to Prof. Morio Tonogi for the opportunity to perform this study, Profs. Masayuki Kobayashi and Satoshi Fujita for their instructions of this study, and colleagues in Department of Pharmacology for their technical advice and assistance.

References

1. Berger T, Borgdorff A, Crochet S, Neubauer FB, Lefort S, Fauvet B et al. (2007) Combined voltage and calcium epifluorescence imaging in vitro and in vivo reveals subthreshold and suprathreshold dynamics of mouse barrel cortex. J Neurophysiol 97, 3751-3762.
2. Chen TW, Wardill TJ, Sun Y, Pulver SR, Renninger SL, Baohan A et al. (2013) Ultrasensitive fluorescent proteins for imaging neuronal activity. Nature 499, 295-300.
3. Dana H, Chen TW, Hu A, Shields BC, Guo C, Looger LL et al. (2014) *Thy1*-GCaMP6 transgenic mice for neuronal population imaging *in vivo*. PLoS One 9, e108697.
4. Huber D, Gutnisky DA, Peron S, O'Connor DH, Wiegert JS, Tian L et al. (2012) Multiple dynamic representations in the motor cortex during sensorimotor learning. Nature 484, 473-478.
5. Kimura R, Safari MS, Mirnajafi-Zadeh J, Kimura R, Ebina T, Yanagawa Y et al. (2014) Curtailing effect of awakening on visual responses of cortical neurons by cholinergic activation of inhibitory circuits. J Neurosci 34, 10122-10133.
6. Fujita S, Yamamoto K, Kobayashi M (2019) Trigeminal nerve transection-induced neuroplastic changes in the somatosensory and insular cortices in a rat ectopic pain model. eNeuro 6, ENEURO.0462-18.2019.
7. Huang L, Ledochowitsch P, Knoblich U, Lecoq J, Murphy GJ, Reid RC et al. (2021) Relationship between simultaneously recorded spiking activity and fluorescence signal in GCaMP6 transgenic mice. Elife 10, e51675.

8. Horinuki E, O'Hashi K, Kobayashi M (2021) In vivo Ca^{2+} imaging of the insular cortex during experimental tooth movement. J Dent Res 100, 276-282.
9. Luo L, Callaway EM, Svoboda K (2018) Genetic dissection of neural circuits: a decade of progress. Neuron 98, 256-281.
10. Zariwala HA, Borghuis BG, Hoogland TM, Madisen L, Tian L, De Zeeuw CI et al. (2012) A Cre-dependent GCaMP3 reporter mouse for neuronal imaging *in vivo*. J Neurosci 32, 3131-3141.
11. Feng G, Mellor RH, Bernstein M, Keller-Peck C, Nguyen QT, Wallace M et al. (2000) Imaging neuronal subsets in transgenic mice expressing multiple spectral variants of GFP. Neuron 28, 41-51.
12. Pan YA, Misgeld T, Lichtman JW, Sanes JR (2003) Effects of neurotoxic and neuroprotective agents on peripheral nerve regeneration assayed by time-lapse imaging *in vivo*. J Neurosci 23, 11479-11488.
13. Jósvay K, Winter Z, Katona RL, Pecze L, Marton A, Buhala A et al. (2014) Besides neuro-imaging, the Thy1-YFP mouse could serve for visualizing experimental tumours, inflammation and wound-healing. Sci Rep 4, 6776.
14. Caroni P (1997) Overexpression of growth-associated proteins in the neurons of adult transgenic mice. J Neurosci Methods 71, 3-9.
15. Notini AJ, Li R, Western PS, Sinclair AH, White SJ (2009) Rapid and reliable determination of transgene zygosity in mice by multiplex ligation-dependent probe amplification. Transgenic Res 18, 987-991.
16. Lopez ME (2012) A quick, no frills approach to mouse genotyping. Bio Protoc 2, e244.

17. Jacquot S, Chartoire N, Piguet F, Hérault Y, Pavlovic G (2019) Optimizing PCR for mouse genotyping: recommendations for reliable, rapid, cost effective, robust and adaptable to high-throughput genotyping protocol for any type of mutation. Curr Protoc Mouse Biol 9, e65.
18. Ohtani S, Fujita S, Hasegawa K, Tsuda H, Tonogi M, Kobayashi M (2018) Relationship between the fluorescence intensity of rhodamine-labeled orexin A and the calcium responses in cortical neurons: an *in vivo* two-photon calcium imaging study. J Pharmacol Sci 138, 76-82.
19. Wang T, Jang WH, Lee S, Yoon CJ, Lee JH, Kim B et al. (2016) Moxifloxacin: clinically compatible contrast agent for multiphoton imaging. Sci Rep 6, 27142.
20. Arras M, Rettich A, Seifert B, Käsermann HP, Rülicke T (2007) Should laboratory mice be anaesthetized for tail biopsy? Lab Anim 41, 30-45.
21. Jerius H, Beall A, Woodrum D, Epstein A, Brophy C (1998) Thrombin-induced vasospasm: cellular signaling mechanisms. Surgery 123, 46-50.
22. Broussard GJ, Liang Y, Fridman M, Unger EK, Meng G, Xiao X et al. (2018) In vivo measurement of afferent activity with axon-specific calcium imaging. Nat Neurosci 21, 1272-1280.
23. Lin X, Zhao T, Xiong W, Wen S, Jin X, Xu XM (2019) Imaging neural activity in the primary somatosensory cortex using *Thy1*-GCaMP6s transgenic mice. J Vis Exp 7, 10.3791/56297.
24. Wolf JA, Stys PK, Lusardi T, Meaney D, Smith DH (2001) Traumatic axonal injury induces calcium influx modulated by tetrodotoxin-sensitive sodium channels. J Neurosci 21, 1923-1930.

25. Stys PK, Waxman SG, Ransom BR (1991) Na^{+}-Ca^{2+} exchanger mediates Ca^{2+} influx during anoxia in mammalian central nervous system white matter. Ann Neurol 30, 375-380.
26. Morley P, Hogan MJ, Hakim AM (1994) Calcium-mediated mechanisms of ischemic injury and protection. Brain Pathol 4, 37-47.
27. Sheldon C, Diarra A, Cheng YM, Church J (2004) Sodium influx pathways during and after anoxia in rat hippocampal neurons. J Neurosci 24, 11057-11069.
28. Havran WL, Allison JP (1990) Origin of Thy-1^{+} dendritic epidermal cells of adult mice from fetal thymic precursors. Nature 344, 68-70.

Figures

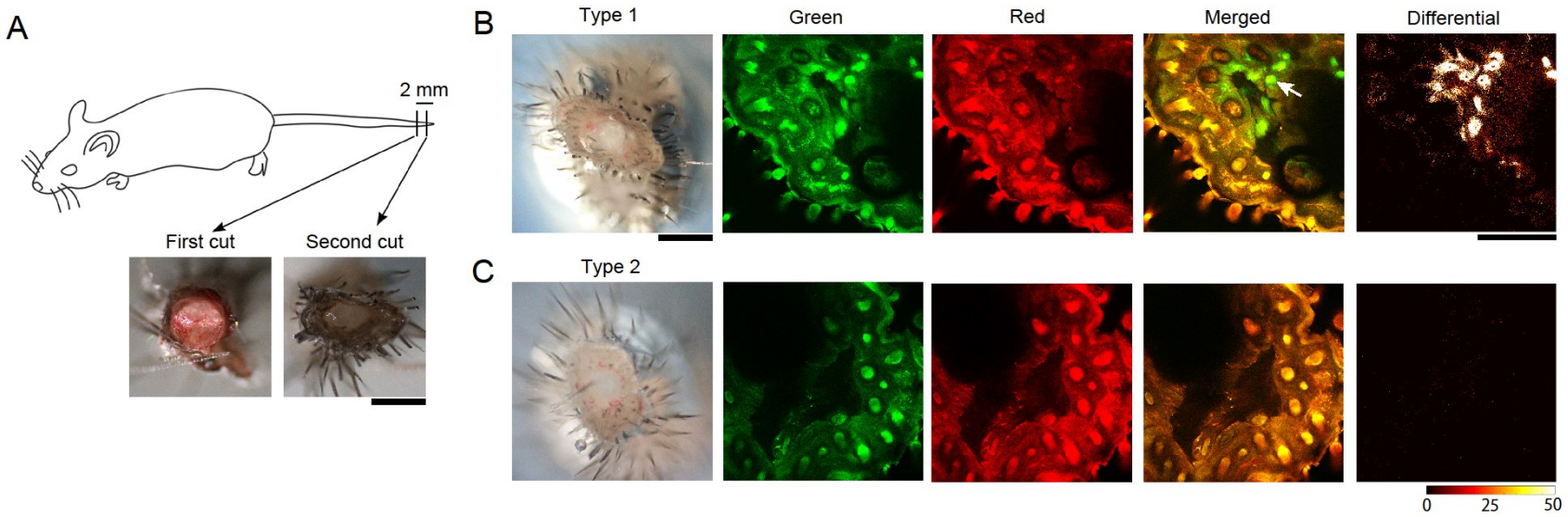

Figure 1. Typical examples for the two types of fluorescent patterns in the cross-sectioned tail. (A) Tail biopsy. Initially, the tail was cut at 2 mm from the tip (the first cut). Then, the resected tail was also cut at the center (the second cut). Note that attached blood was found in the proximal plane (the first cut), but little in the distal plane (the second cut). (B, C) Macroscopic pictures, emitted green light images, emitted red light images, merged images, and differential images (subtracted the intensity of red light from the intensity green light) were arranged in type 1 example (B; the presence of green fluorescence) and type 2 example (C; the absence of green fluorescence). Arrow indicates an area of green fluorescence only. The differential value of each pixel in differential images is color-coded, and the brightest pixels are exceeding 50 in differential value. Note that some structures with high green light intensity were clearly visible in the merged image in type 1, but not in type 2. Scale bars in the macroscopic pictures and other images are 500 μm and 200 μm, respectively.

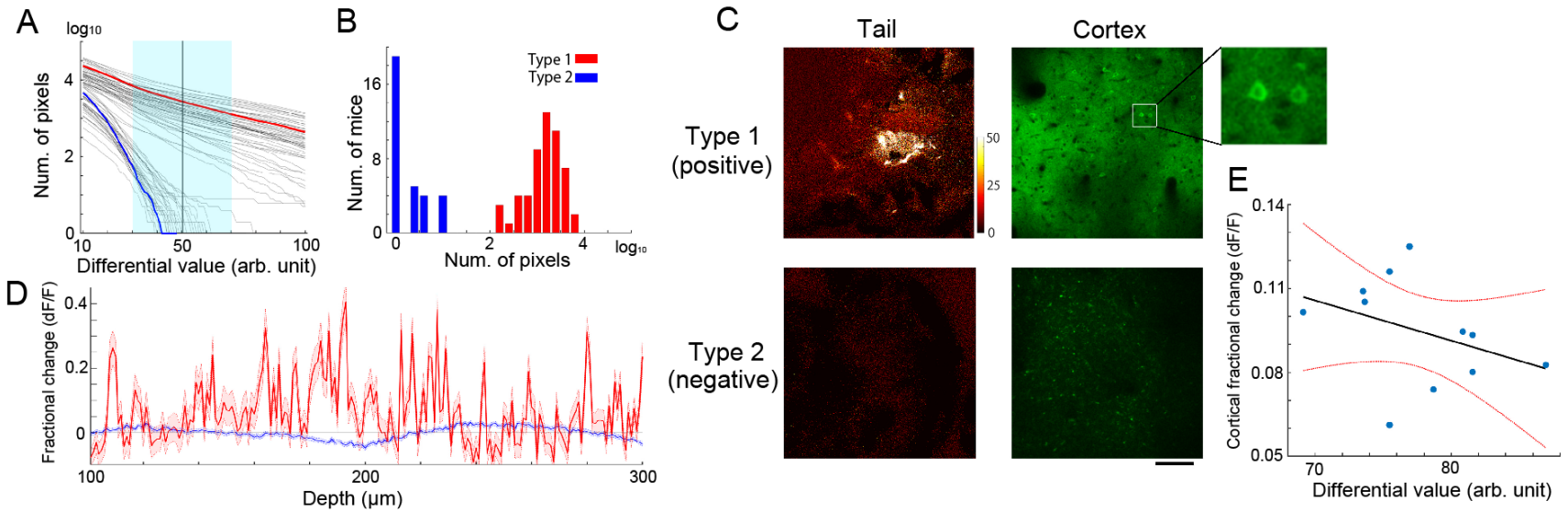

Figure 2. Quantitative screening of the two types of fluorescent patterns and identification of the cortical GCaMP6s expression. (A) Change in the number of pixels exceeding the differential values from 10 to 100 in each cross-sectioned image (N = 86). At the differential values from 30 to 70 (area shaded in cyan), k-means clustering yields identical screening results. The red (type 1) and blue (type 2) lines indicate typical examples shown in C and D. (B) An example of the clustering results at 50 in the differential value (vertical line in A). (C) Examples of differential images from the tail (left panels) and green fluorescence images from the cerebral cortex (right panels) in type 1 and 2. The enlarged square highlights spontaneously activating two neurons. The scale bar is 100 μm. (D) Examples of the fluorescent depth profiles from two types of animals. Solid and dashed lines indicate the mean and SEM, respectively (red, type 1; blue type 2). Their transition was statistically significant (n = 301, P < 0.001, Mann–Whitney U test). (E) Relationship between the tail and cortical fluorescent intensity. Whether the cortical fluorescence has a positive relationship to the fluorescent intensity of cross-sectioned tail was analyzed by linear regression. The overall regression was not statistically significant (N = 11, F(1, 9) = [1.44], P = 0.26), suggesting no relationship between them. Blue points indicate the mean of cortical fluorescence and the differential value of the cross-sectioned tail in each mouse. The black and red lines indicate the regression line and the 95% confidence interval, respectively.

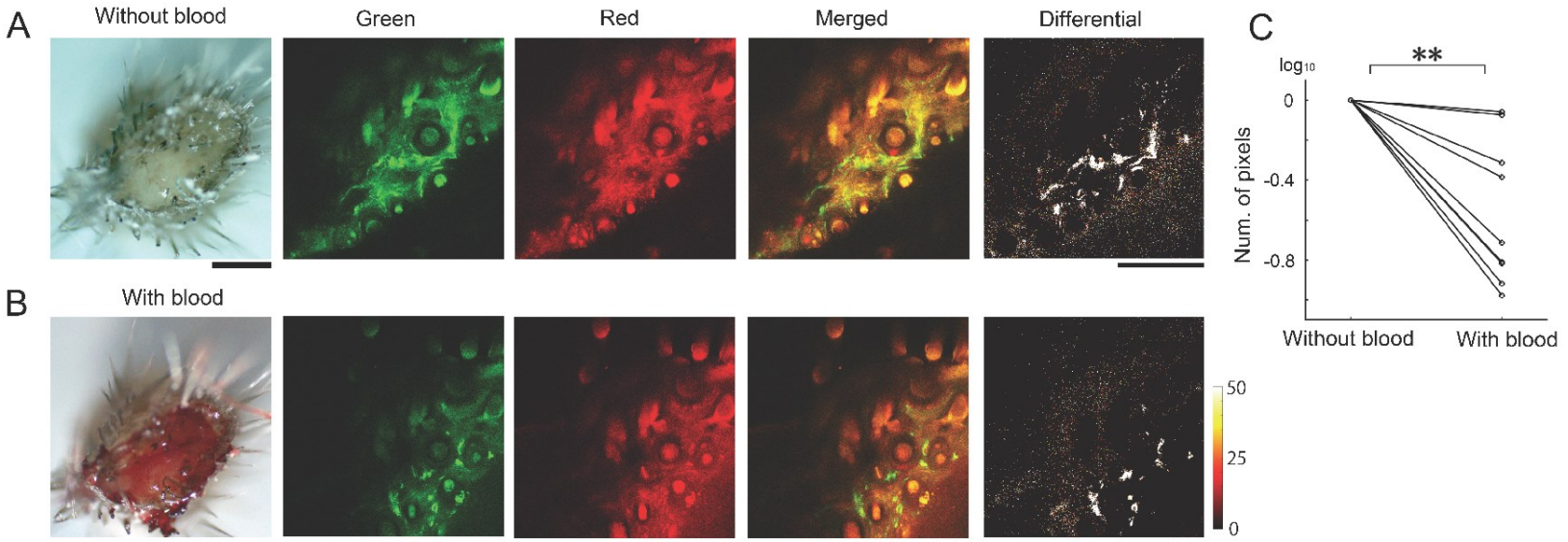

Figure 3. The attached blood reduces the fluorescent intensity from the cross-sectioned tail. Typical examples for the cross-sectioned tail images without (A) and with (B) blood for an identical GCaMP6s-positive sample. Macroscopic pictures, emitted green light images, emitted red light images, merged images, and differential images are shown. The differential value of each pixel in differential images is color-coded. (C) A comparison of the number of pixels exceeding the differential value of 50 between with- and without-attached blood for identical GCaMP6s-positive samples (n = 9, $^{**}P < 0.01$, Wilcoxon signed-rank test). The different fluorescent patterns depending on with- or without-attached blood possibly yield erroneous screening results. Scale bars in the macroscopic pictures and other images are 500 μm and 200 μm, respectively.

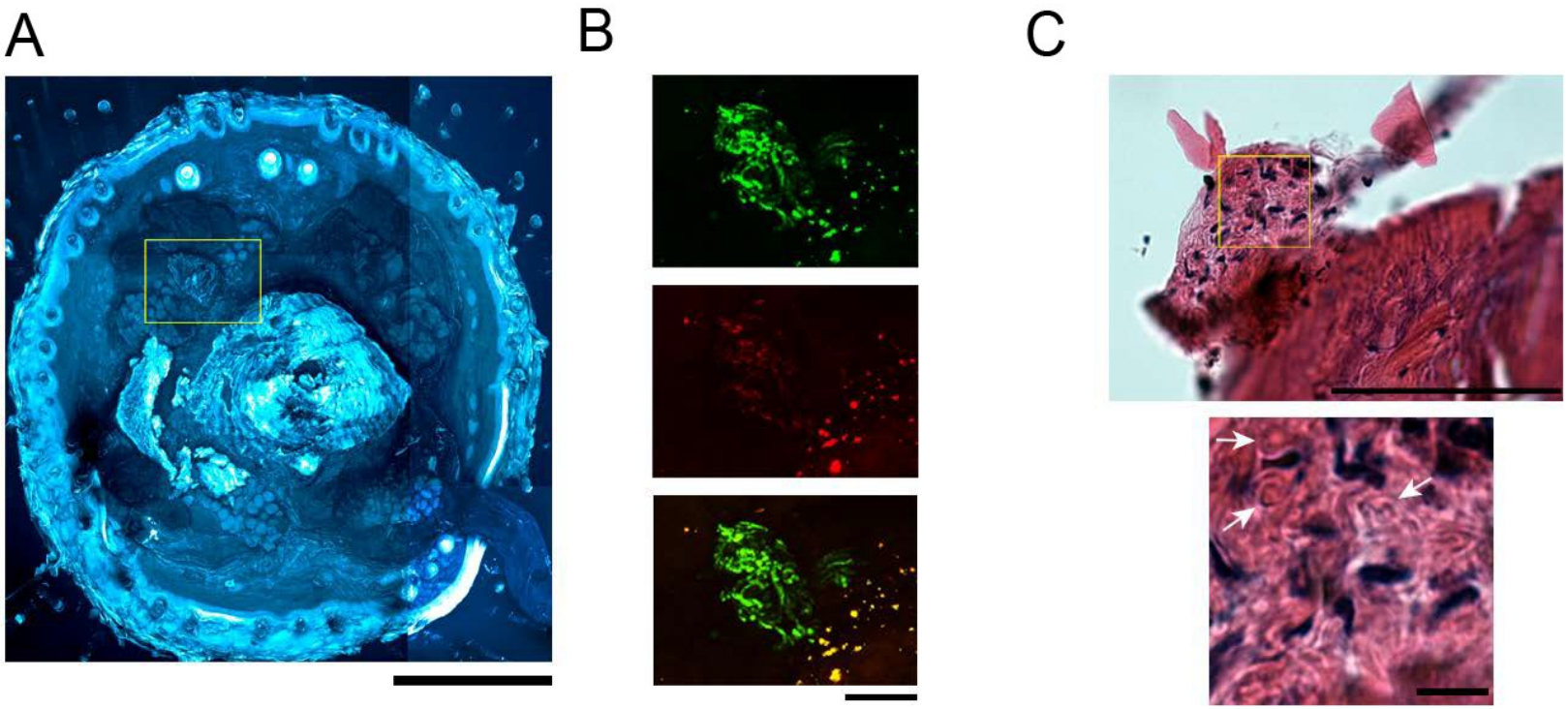

Figure 4. Confirmation of the origin of the green fluorescence. (A) An entire cross-sectioned tail image contrasted by moxifloxacin. (B) Fibrous structures emitting strong green fluorescence imaged from the rectangle in A. (C) Hematoxylin and eosin (H-E) staining of the imaged sample. Lower panel shows the magnified image of the box in the upper panel. Arrows indicate the axons. Scale bars in A, B, C (upper pane), and C (lower pane) are 500, 100, 100, and 10 μm, respectively.

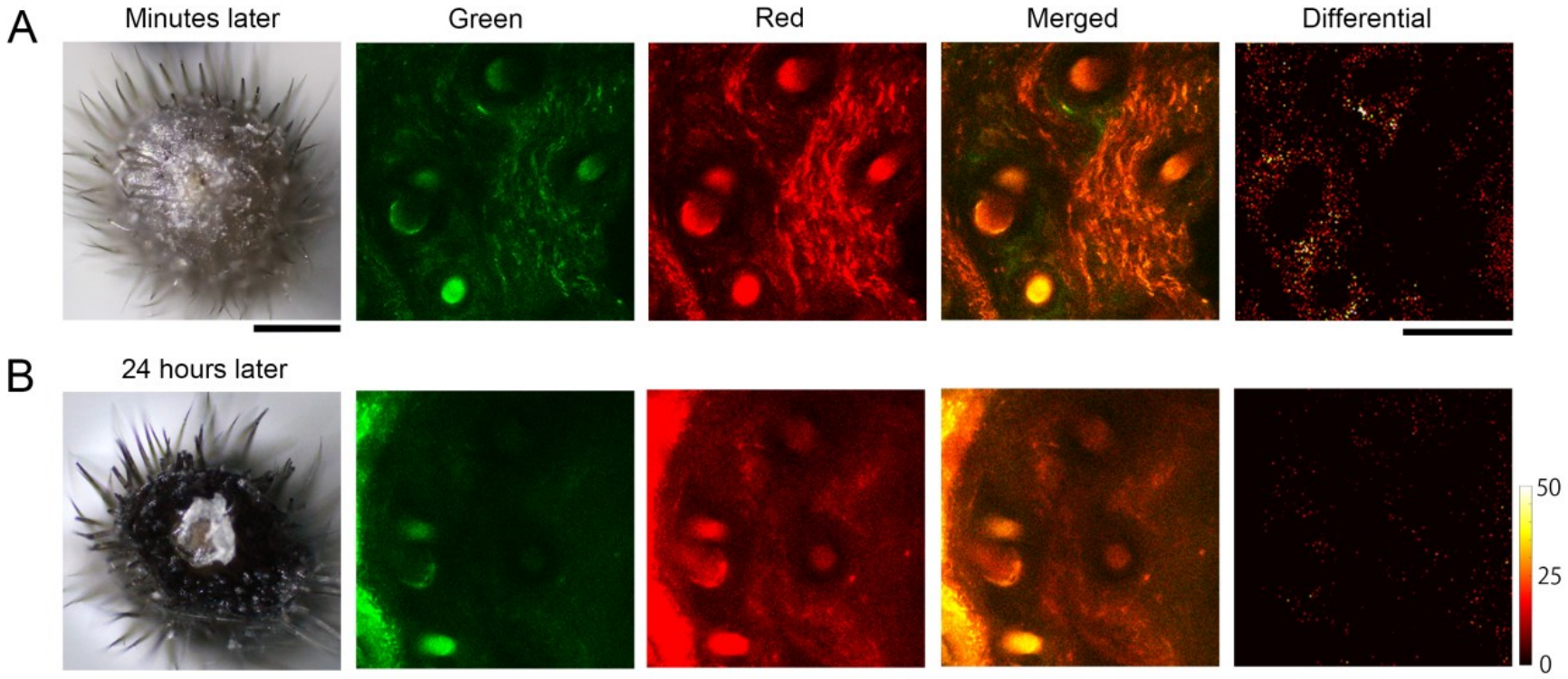

Figure 5. Reduction of the intensity of green fluorescence in the cross-sectioned tail after 24 h. (A) Images minutes after the tail resection. (B) Images 24 h after the tail resection. The pixel value is color-coded in differential images, at which the brightest pixels correspond to the deferential fluorescence exceeding 50 in the threshold value. Note that some structures with green fluorescence intensity were clearly visible in the merged image in A, but not in B. Scale bars in the macroscopic pictures and other images are 500 μm and 100 μm, respectively.